Chemistry & Biology
Article

# Identification and Evaluation of Small Molecule Pan-Caspase Inhibitors in Huntington's Disease Models

Melissa J. Leyva,[1] Francesco DeGiacomo,[2] Linda S. Kaltenbach,[3] Jennifer Holcomb,[2] Ningzhe Zhang,[2] Juliette Gafni,[2] Hyunsun Park,[4] Donald C. Lo,[3] Guy S. Salvesen,[5] Lisa M. Ellerby,[2,*] and Jonathan A. Ellman[6,*]
[1]Department of Chemistry, University of California, Berkeley, CA 94720, USA
[2]Buck Institute for Age Research, Novato, CA 94945, USA
[3]Duke University Medical Center, Durham, NC 27704, USA
[4]CHDI Foundation Inc., Los Angeles, CA 90045, USA
[5]Burnham Institute for Medical Research, La Jolla, CA 92037, USA
[6]Department of Chemistry, Yale University, New Haven, CT 06437, USA
*Correspondence: lellerby@buckinstitute.org (L.M.E.), jonathan.ellman@yale.edu (J.A.E.)
DOI 10.1016/j.chembiol.2010.08.014

## SUMMARY

**Huntington's Disease (HD) is characterized by a mutation in the huntingtin (Htt) gene encoding an expansion of glutamine repeats on the N terminus of the Htt protein. Numerous studies have identified Htt proteolysis as a critical pathological event in HD postmortem human tissue and mouse HD models, and proteases known as caspases have emerged as attractive HD therapeutic targets. We report the use of the substrate activity screening method against caspase-3 and -6 to identify three novel, pan-caspase inhibitors that block proteolysis of Htt at caspase-3 and -6 cleavage sites. In HD models these irreversible inhibitors suppressed *Hdh*$^{111Q/111Q}$-mediated toxicity and rescued rat striatal and cortical neurons from cell death. In this study, the identified nonpeptidic caspase inhibitors were used to confirm the role of caspase-mediated Htt proteolysis in HD. These results further implicate caspases as promising targets for HD therapeutic development.**

## INTRODUCTION

Huntington's disease (HD) is a dominantly inherited neurodegenerative disorder characterized by progressive deterioration of neurons in the striatum and cortex. Symptoms can occur at any age but usually occur with an adult-onset, and patients exhibit progressive loss of cognitive and motor function. HD is caused by a mutation in the Htt gene with a trinucleotide (CAG) expansion encoding glutamine repeats in the N terminus of huntingtin (Htt), a scaffold protein with many interacting proteins that has been shown to be involved in vesicular trafficking (HDCRG, 1993). A neuropathological hallmark of HD in human and mouse models is the accumulation of N-terminal Htt fragments leading to cytotoxicity, suggesting that Htt proteolysis is a critical event in pathogenesis (Davies et al., 1997; DiFiglia et al., 1997; Gafni and Ellerby, 2002; Gafni et al., 2004; Goldberg et al., 1996; Gutekunst et al., 1999; Martindale et al., 1998).

Numerous studies have demonstrated the cleavage of Htt by multiple proteases, including aspartyl proteases, calpains, and caspases (Gafni and Ellerby, 2002; Gafni et al., 2004; Goldberg et al., 1996; Lunkes et al., 2002; Wellington et al., 1998). Caspases are cysteine proteases characterized by their high specificity for substrates with an aspartic acid at the site of cleavage in the P1 position and play a prominent role in apoptosis (Pop and Salvesen, 2009). Dysregulation of apoptosis has been implicated in stroke, neuronal degeneration, liver disease, cancer, and autoimmune disorders (Reed, 2002). Due to the dramatic neuronal cell death in HD, it is not surprising that Htt was the first neuronal protein identified as a caspase substrate (Goldberg et al., 1996). A number of studies have defined the cleavage sites of Htt for caspase-3 at amino acids 513 and 552, for caspase-2 at amino acid 552, and for caspase-6 at amino acid 586 (Hermel et al., 2004; Wellington et al., 1998, 2000). Recently, caspase-6 cleavage of mutant Htt and activation of caspase-6 have been shown to play a significant role in HD pathogenesis in HD mouse models (Hermel et al., 2004; Graham et al., 2006). Caspase-6 is also activated in HD postmortem tissue (Hermel et al., 2004).

Although the aforementioned studies clearly implicate caspase-mediated cleavage of Htt in HD, few studies have evaluated the effects of caspase inhibition on HD cell death. The nonspecific irreversible, peptidic fluoromethyl ketone inhibitor, zVAD-fmk, protected striatal neurons against malonate-induced excitotoxicity (Schulz et al., 1998), and the reversible caspase-3 specific inhibitor, M826, significantly displayed neuroprotection against malonate-induced striatal injury in a rat model of HD (Toulmond et al., 2004). Additionally, through indirect means minocycline, a tetracycline derivative with the ability to cross the blood-brain barrier, inhibits caspase-1 and caspase-3 transcriptional upregulation and delays cell death in HD transgenic mouse models (Chen et al., 2000). The development of small molecule, nonpeptidic inhibitors of both caspase-3 and -6 and their evaluation in HD biology would provide useful tool compounds to the field. Unfortunately, whereas numerous caspase inhibitors have been developed (Cornelis et al., 2007; O'Brien and Lee, 2004), most are peptidic in nature, and efficacy

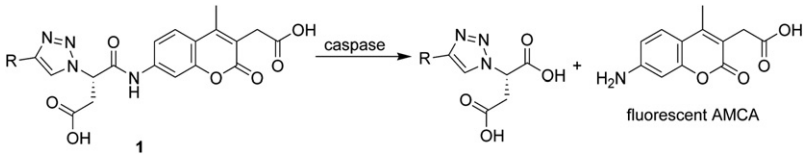


**Figure 1. Screening of AMCA Substrates 1**
First step in SAS method, screening diverse AMCA substrates against caspase to yield a fluorescent AMCA reporter group.

in cells and animals is compromised due to poor cell penetration and absorption, distribution, metabolism, and excretion (ADME) properties, respectively (Talanian et al., 1997). Therefore, we applied a substrate-based fragment approach called substrate activity screening (SAS) to the development of nonpeptidic inhibitors of caspase-3 and -6. In the SAS method, which has previously been applied to proteases of the papain family (Brak et al., 2008; Inagaki et al., 2007; Patterson et al., 2006; Wood et al., 2005), weak binding nonpeptidic substrate fragments are identified, optimized, and then converted to potent inhibitors. Herein, we report the identification of three novel, nonpeptidic pan-caspase irreversible inhibitors that blocked proteolysis of Htt at caspase-3 and caspase-6 sites, suppressed *Hdh*$^{111Q/111Q}$-mediated toxicity, and rescued HttN90Q73-induced degeneration of rat striatal and cortical neurons.

## RESULTS AND DISCUSSION

### Substrate Library Synthesis and Screening

To target caspase-3, we initially set out to create a library that incorporated the P1 aspartic acid required for caspase recognition and amide bond hydrolysis. To satisfy the goal of identifying nonpeptidic fragments, we synthesized an initial library of 1,4-disubstituted-1,2,3-triazole substrates **1** (Figure 1) because triazoles have been demonstrated as efficient amide bond replacements in the development of protease inhibitors (Brik et al., 2005; Wood et al., 2005), and diverse functionality could readily be introduced into the substrates using solid-phase methods (see Supplemental Experimental Procedures available online). Substrates were screened in a high-throughput fluorometric assay to detect caspase-3-catalyzed amide bond proteolysis and liberation of the fluorophore, 7-amino-4-methylcoumarin-3-acetic acid (AMCA) (Figure 1).

### Structure-Activity Relationship of AMCA Substrates against Caspase-3

Figure 2A exhibits the relative cleavage efficiencies of a subset of initial substrates that were evaluated. Substrate **2** with a phenylethyl group at the R position had the lowest cleavage efficiency of all of the substrates for which turnover was detected and was assigned a relative cleavage efficiency value of 1.0. Substrates for which no turnover was detected were given a relative cleavage efficiency value of zero. Substrates **8** and **9** with $\alpha$-branching at the R position as provided by the cyclohexyl moiety along with hydroxyl and amide groups, respectively, that are both capable of H bonding, showed the highest activity. Substrate **9** was particularly appealing because the amine functionality provides the opportunity to introduce a variety of additional functionality through amine acylation and reductive amination chemistry.

To further explore the effect of $\alpha$-branched substituents within the amide framework present in substrate **9**, an additional collection of substrates was prepared and evaluated (Figure 2B). When the cyclohexyl group that introduces $\alpha,\alpha$-dibranching in substrate **9** was replaced by the $\alpha$-monobranched structures in substrates **10**–**13**, no substrate turnover was observed, which suggests the importance of maintaining dibranched functionality at this position. Similarly, dibranched substituents with the smaller methyl, ethyl, and isopropyl groups all displayed reduced cleavage efficiency (substrates **14**–**17**). In contrast, substrate **18**, which incorporated methyl and cyclohexyl substituents with an (*S*)-configuration, showed a greater than 5-fold increase in cleavage efficiency relative to the initial cyclohexyl amide substrate **9**. It is noteworthy that caspase-3 showed very strong chiral recognition with no cleavage observed for substrate **19**, which is the (*R*)-epimer of substrate **18**. The strong preference for the (*S*)-epimer suggests the importance of this configuration for proper orientation and enhanced binding in the S2 pocket of caspase-3.

With substrate **18** incorporating cyclohexyl and methyl substituents with (*S*)-configuration providing the highest cleavage efficiency, we next chose to evaluate the replacement of the acetamide group with a variety of different amides and amines to identify key binding interactions for this region of the substrate (representative structures shown in Figure 2C). Replacing the acetamide in substrate **18** with the *N*,*N*-diethyl moiety in substrate **20** almost completely eliminated substrate turnover, suggesting the importance of the H-bond donor or accepting capability of the amide functionality. In contrast, replacing the acetamide in substrate **18** with the benzamide in substrate **21** resulted in only a modest reduction in cleavage efficiency, demonstrating that groups considerably larger than acetamide can be accommodated in the enzyme active site. The isosteric secondary amine in substrate **22** resulted in a >10-fold reduction in cleavage efficiency of the substrate, again confirming the importance of the amide functionality either for orientation or for hydrogen-bonding interactions. The phenyl acetamide present in substrate **23** resulted in a modest increase in cleavage efficiency, whereas the isosteric phenylmethylsulfonamide present in **24**, which maintains hydrogen-bond donor and accepting capability, provided a considerable boost in cleavage efficiency. Finally, introduction of a second carboxylic acid in substrates **25** and **26** resulted in a considerable increase in cleavage efficiency, with substrate **25** providing the highest cleavage efficiency out of all the substrates tested. This result is consistent with the known peptide substrate specificities for many of the caspases, which prefer a second aspartic acid residue at the P4 position, i.e., four amino acids away from the cleavage site (Talanian et al., 1997).

### Substrate Screening and Optimization against Caspase-6

For peptide substrates, caspase-3 and -6 both require an aspartic acid residue at the site of cleavage but differ in preferred

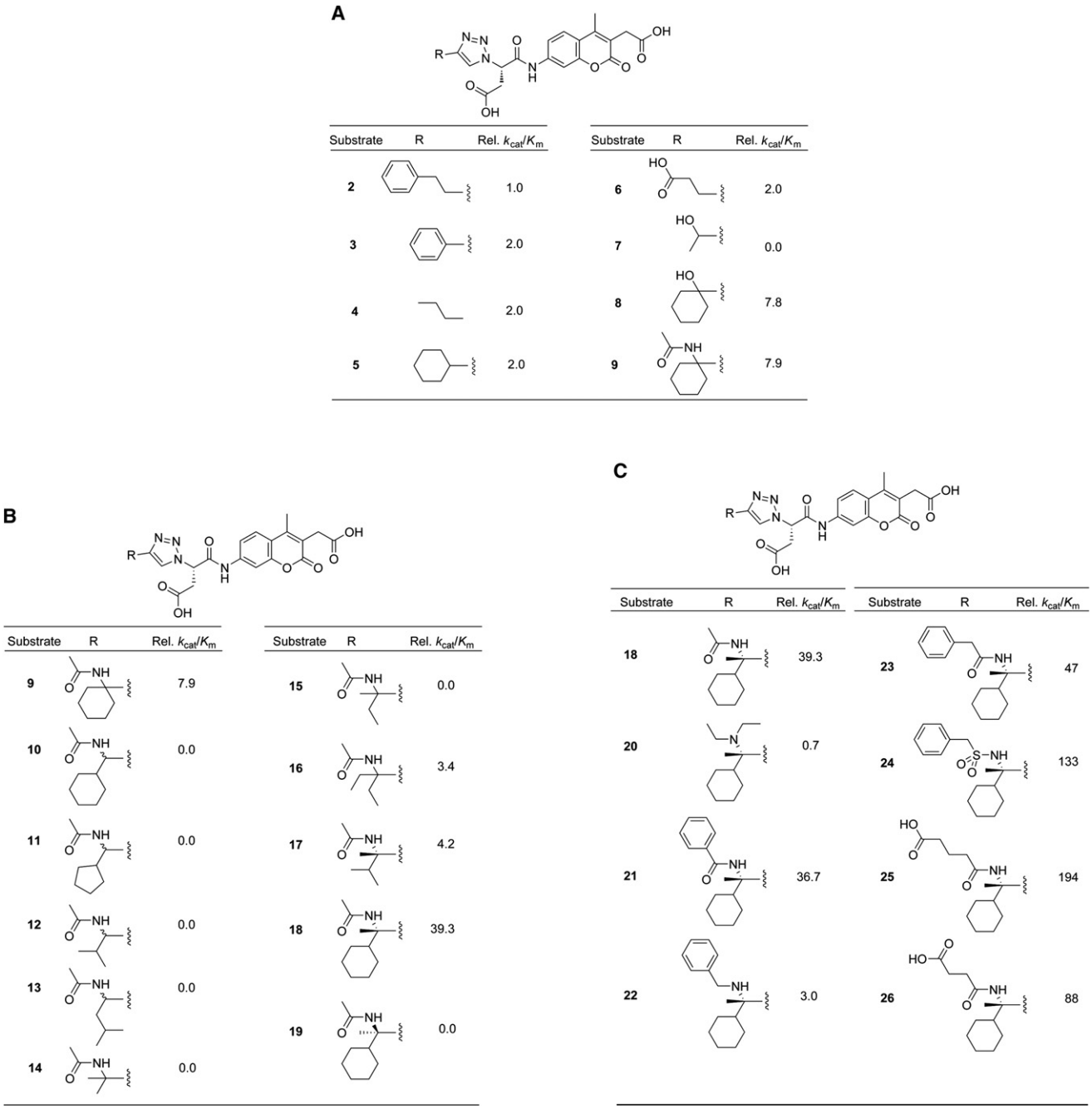


**Figure 2. Caspase-3 Cleavage Efficiencies of AMCA Substrates**

(A) Relative $k_{cat}/K_m$ of initial substrate library incorporating alkyl and polar R groups. The relative $k_{cat}/K_m$ of the least efficiently cleaved substrate for which turnover could be detected was assigned a value of 1.0. For caspase-3, substrate **2** was assigned a value of 1.0.

(B) Relative $k_{cat}/K_m$ of substrate set incorporating α-substituted amide R structures.

(C) Relative $k_{cat}/K_m$ of *N*-substituted amide substrates with (*S*)-configured methyl and cyclohexyl substituents.

See also Figure S1.

amino acid side chains two (P2) and four (P4) amino acids from the cleavage site (Thornberry et al., 1997). In P2, caspase-3 shows a strong preference for small hydrophobic residues, whereas caspase-6 tolerates larger residues. In P4, caspase-3 demonstrates an almost absolute requirement for an aspartic acid residue, whereas larger aliphatic residues are tolerated by caspase-6. Therefore, all of the previously synthesized caspase-3 substrates were assayed against caspase-6 with key substrate activity relationships represented by the substrates shown in Figure 3A. No substrate turnover was observed for α-monobranched substrates, as exemplified by substrates **10** and **13**, therefore, they were given the relative cleavage

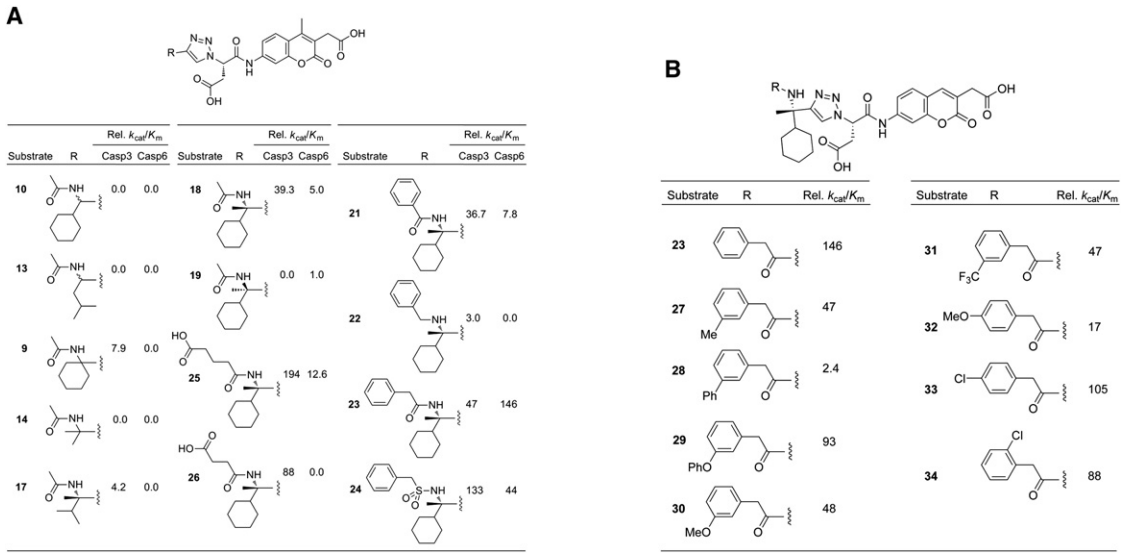


**Figure 3. Caspase-3 and -6 Cleavage Efficiencies of AMCA Substrates**

(A) Relative $k_{cat}/K_m$ of a select number of previously synthesized AMCA substrates against caspase-3 and -6. The relative $k_{cat}/K_m$ of the least efficiently cleaved substrate for which turnover could be detected was assigned a value of 1.0. For caspase-3, substrate **2** was assigned a value of 1.0 (Figure 2A). For caspase-6, substrate **19** was assigned a value of 1.0.

(B) Relative $k_{cat}/K_m$ of newly synthesized substituted phenylamide substrates against caspase-6.

efficiencies of zero. Out of all the α, α-dibranched substrates, only substrates **18** and **19** with methyl and cyclohexyl substituents resulted in cleavage. Substrate **19** gave the lowest cleavage efficiency out of all the substrates for which turnover was detected for caspase-6 and was assigned a relative cleavage efficiency of one. The (*S*)-epimer of substrate **18** provided a 5-fold increase in cleavage efficiency relative to substrate **19**, consistent with the stereochemical preference observed for caspase-3. For substrate **25**, incorporating the carboxylic acid functionality resulted in a greater than 2-fold increase in cleavage efficiency, whereas no substrate turnover was detected for substrate **26**, which also contains the carboxylic functionality but with a shorter chain length. The importance of the H-bond accepting capability of the amide carbonyl is apparent by comparing the cleavage rate of amide substrate **21** and amine substrate **22**. The phenylacetamide substrate **23** provided a considerable increase in cleavage efficiency, with the corresponding isosteric phenylmethylsulfonamide substrate **24** also serving as a good substrate but with ~3-fold lower efficiency than **23**.

Figure 3A displays notable differences in SARS between caspase-3 and caspase-6 substrates. The chiral preference for (*S*)-epimer **18** was stronger for caspase-3 over caspase-6. This can be explained by the difference in size of the S2 pocket between caspase-3 and caspase-6. Various substitutions are tolerated in P2 for both caspases, but caspase-6 is able to accommodate larger aliphatic and aromatic residues in contrast to caspase-3. A difference in relative cleavage efficiencies between benzamide **21** and phenylacetamide **23** was observed for caspase-3 and caspase-6. Substrate **23** showed only a modest increase in cleavage efficiency compared to substrate **21** for caspase-3, whereas **23** displayed a >18-fold increase compared to **21** for caspase-6. Consistent with the known peptidic substrate specificity data for caspase-3 and -6 (see above), substrate **25** with an acidic side chain capable of binding in the S4 pocket was the most efficiently cleaved by caspase-3; whereas substrate **23** displaying hydrophobic functionality was the most efficiently cleaved by caspase-6.

Because substrate **23** incorporating the phenylacetamide showed by far the greatest cleavage efficiency by caspase-6, analogs with substitution on the phenyl ring were prepared and evaluated (Figure 3B). Methyl and phenyl electron-donating substituents at the *meta* position in substrates **27** and **28** decreased cleavage efficiency. The considerably lower cleavage efficiency of substrate **28** can be attributed to unfavorable steric interactions with the large phenyl substituent. Modest reductions in cleavage efficiency were also observed for substrates with meta-substitution, with the more strongly electron-donating phenoxy and methoxy substituents, **29** and **30**, respectively, as well as with the electron-withdrawing trifluoromethyl substituent (substrate **31**). The electron-donating methoxy substituent at the *para* position provided an ~8-fold drop in cleavage efficiency (substrate **32**). A slight decrease in cleavage efficiency was also observed for the electron-withdrawing chloro substituent at both the *para* and *ortho* positions, present in substrates **33** and **34**, respectively.

## Inhibitor Synthesis and Screening

The final step in the SAS method is conversion of the most active substrates to inhibitors. Substrate cleavage is only observed when the amide carbonyl of the *N*-acyl aminocoumarin is properly positioned in the enzyme active site, thus allowing for the aminocoumarin group to be replaced by a mechanism-based pharmacophore to produce reversible or irreversible inhibitors. Pharmacophore selection was based upon a class of peptidic pan-caspase inhibitors containing the 2,3,5,6-tetrafluorophenoxy ketone irreversible inhibitor pharmacophore

A

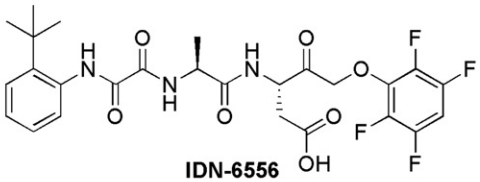


B

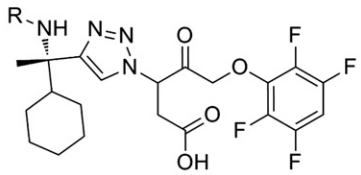

R =

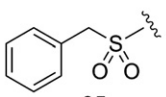
35

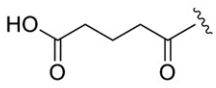
36

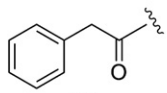
37

| | 35 | 36 | 37 |
|---|---|---|---|
| caspase 1 | 55,200 ± 2,600 | 243,250 ± 350 | 55,200 ± 200 |
| caspase 2[b] | 33.0 ± 0.5 | 2.0 ± 0.1 | 6.90 ± 0.3 |
| caspase 3 | 47,000 ± 1,400 | 81,700 ± 6,900 | 29,850 ± 850 |
| caspase 6 | 23,100 ± 1,900 | 32,950 ± 1,650 | 45,750 ± 450 |
| caspase 7 | 27,700 ± 2,000 | 57,250 ± 1,550 | 34,200 ± 3,800 |
| caspase 8 | 82, 850 ± 1,150 | 30, 650 ± 1,950 | 60,000 ± 2,800 |
| caspase 9 | 18,250 ± 4,050 | 7,550 ± 1,650 | 28,100 ± 2,500 |
| cathepsin B[c] | no inhibition | no inhibition | no inhibition |
| cathepsin S | 1,138 ± 526 | 331 ± 44 | 535 ± 44 |
| cathepsin V[c] | no inhibition | no inhibition | no inhibition |
| legumain | not detected[d] | not detected[d] | no inhibition[c] |

**Figure 4. Irreversible 2,4,5,6-Tetrafluorophenoxymethyl Inhibitors**

(A) Pan-caspase inhibitor incorporating a 2,4,5,6-tetrafluorophenoxymethyl ketone pharmacophore developed by Idun Pharmaceuticals.

(B) Inactivation rates of irreversible 2,4,5,6-tetrafluorophenoxymethyl inhibitors against caspases 1–3 and 5–9, cathepsins B, S, and V, and legumain. [a]Assays determining $k_{inact}/K_i$ ($M^{-1}s^{-1}$) were performed in duplicate with SD values included. [b]Caspase-2 assays determining $k_{inact}/K_i$ ($M^{-1}s^{-1}$) were performed in duplicate with SD values included. [c]No inhibition after 15 min of preincubation with various concentrations of inhibitor of up to 400 μM. [d]Very weak inhibitory activity prevented determination of $k_{inact}/K_i$ values, but $IC_{50}$ values of 200–350 mM were obtained after 15 min of preincubation.

See also Figures S2–S4.

developed by Idun Pharmaceuticals because members of this inhibitor series have advanced the farthest in clinical development (Linton et al., 2004, 2005). Indeed, inhibitor **IDN-6556** (Figure 4A) was determined to be nontoxic in mouse models and has entered Phase II clinical trials for the treatment of human liver preservation injury (Baskin-Bey et al., 2007). The 2,3,5,6-tetrafluorophenoxyketone pharmacophore was incorporated into three distinct substrates, **23–25**, that showed good cleavage efficiency by both caspase-3 and -6 to provide inhibitors **35–37** (see Supplemental Experimental Procedures for inhibitor synthesis and characterization). The inhibitory activity of these compounds was then characterized against a full panel of caspases 1–3 and 6–9 (Figure 4B). All three inhibitors provided potent inhibition of caspases 3 and 6, with $k_{inact}/K_i$ values of >20,000 $M^{-1}s^{-1}$ for each enzyme. Each of the inhibitors also provided potent inhibition of caspases 1 and 7–9, as would be expected by the similar substrate specificities across these enzymes. In contrast to the other caspases, caspase-2 has an extended binding pocket, and a P5 residue has been shown to be critical for increased cleavage efficiency (Schweizer et al., 2003; Talanian et al., 1997). Due to this extended binding requirement, it is not surprising that for inhibitors **35–37** poor inhibition of caspase-2 was observed with $k_{inact}/K_i$ values of <33 $M^{-1}s^{-1}$.

Recent studies have demonstrated that incorporation of P1 aspartyl side chain functionality in caspase inhibitors does not necessarily afford selective caspase inhibition. Aspartyl peptidyl fluoromethyl and chloromethyl ketones have been reported to efficiently inhibit other cysteine proteases such as cathepsin B, S, and V as well as legumain (Rozman-Pungercar et al., 2003). More recently, aspartyl peptidic acyloxymethyl ketones have been utilized as efficient cell-permeable activity-based probes for legumain (Sexton et al., 2007). Due to the aforementioned studies, all three inhibitors were screened against multiple cathepsins and legumain to evaluate cross-reactivity. Inhibitors **35–37** displayed no inhibition of cathepsins B and V. Weak inhibition was observed for cathepsin S, with $k_{inact}/K_i$ values of <1138 $M^{-1}s^{-1}$. Inhibition of legumain by **35** and **36** was so poor ($IC_{50}$ = 200–350 μM at 15 min preincubation) that $k_{inact}/K_i$ values could not be calculated, and for inhibitor **37** absolutely no inhibition of this enzyme could be detected. Overall, the caspase-designed aryloxymethyl ketone irreversible inhibitors showed little to no inhibition against legumain, cathepsin B, S, and V.

## Evaluating Inhibitors in HD Models

In vitro, Htt is preferentially cleaved at amino acid 552 by caspase-2, 513 by caspase-3, and 586 by caspase-6 (Hermel

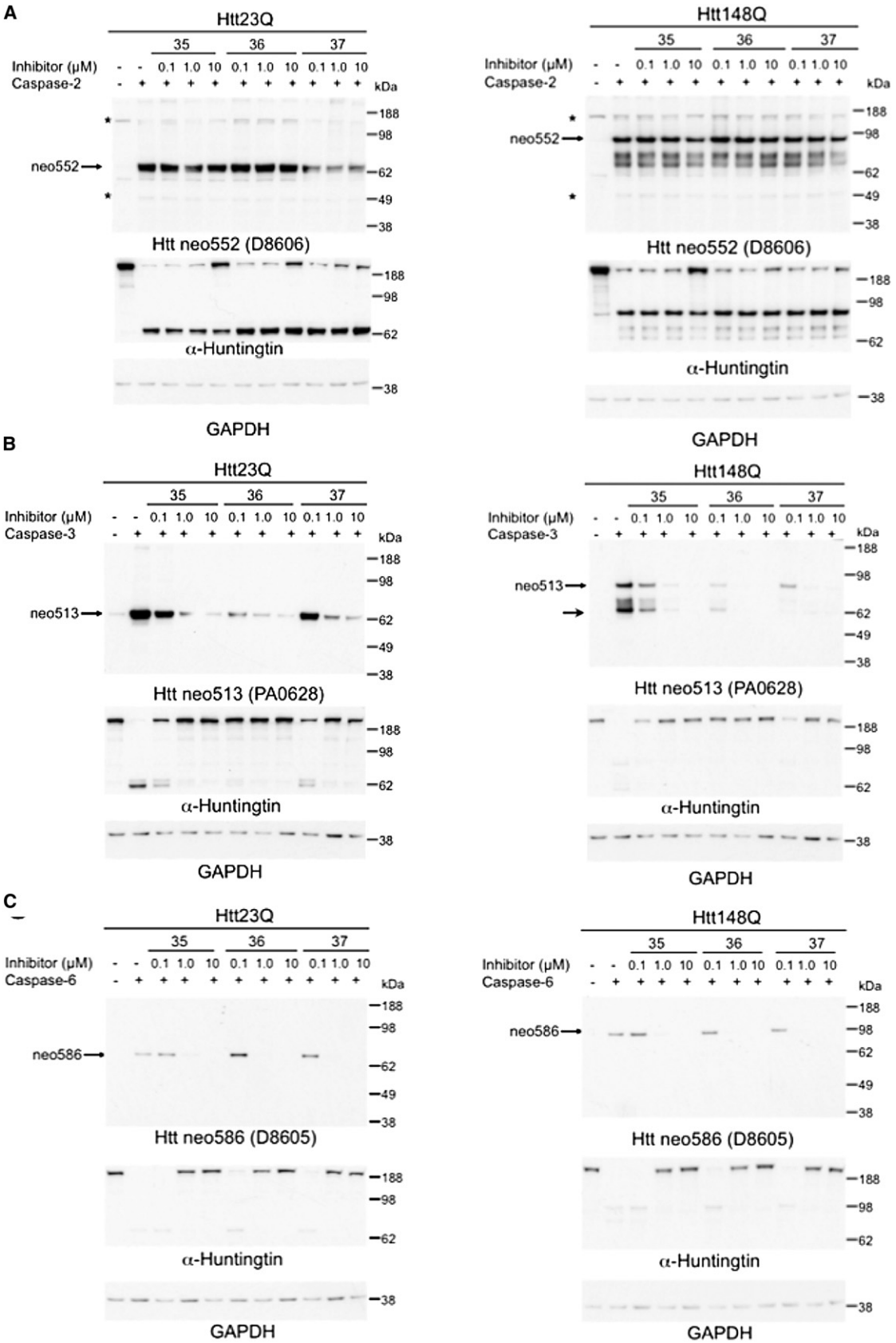
A
Htt23Q
Htt148Q
35
36
37
Inhibitor (μM) - - 0.1 1.0 10 0.1 1.0 10 0.1 1.0 10
Caspase-2 - + + + + + + + + + +
kDa
188
98
62
49
38
neo552
Htt neo552 (D8606)
α-Huntingtin
GAPDH
B
Caspase-3
neo513
Htt neo513 (PA0628)
C
Caspase-6
neo586
Htt neo586 (D8605)

et al., 2004; Wellington et al., 2000). Inhibitors **35**–**37** were each evaluated for Htt proteolysis by caspase-2, -3, and -6 with neo-epitope antibodies that recognize the specific Htt cleavage products using an in vitro assay. Figure 5 shows western blot analysis of cellular lysates expressing full-length Htt23Q and Htt148Q treated with caspase-2, -3, and -6 and the three inhibitors at various concentrations using the neo-specific Htt antibodies. Although minimal protection against cleavage of Htt by caspase-2 was observed as expected (Figure 5A), inhibitors **35**–**37** each effectively blocked proteolysis by caspase-3 at amino acid 513 at all of the tested concentrations (0.1, 1.0, and 10 μM) (Figure 5B). For full-length Htt treated with caspase-6, all three inhibitors, **35**–**37**, also showed complete protection from cleavage at amino acid 586 at concentrations of 1.0 and 10 μM (Figure 5C). To gain insight into the efficiency of the inhibitors for blocking caspase cleavage of Htt, we determined the $k_{cat}/K_m$ of full-length Htt with caspase-3 and caspase-6 (Table S1), and it appears that Htt in lysates is less efficiently cleaved by caspase-6 than caspase-3. This may correlate with the higher dose required to inhibit caspase-6 cleavage of Htt; however, without determining $K_m$ of Htt, we cannot compare the efficiency of the inhibitors for the caspases.

Next, each inhibitor was evaluated in a HD cellular toxicity model by measuring caspase activity and Htt proteolysis. Because HD primarily affects striatal and cortical neurons, we used immortalized mouse striatal cell $Hdh^{7Q/7Q}$ and $Hdh^{111Q/111Q}$ lines to measure cellular toxicity and Htt proteolysis (Trettel et al., 2000). We cultured $Hdh^{7Q/7Q}$ and $Hdh^{111Q/111Q}$ cells and evaluated Htt proteolysis 24 hr after serum withdrawal. We found that the neoHtt513 antibody detected proteolysis of Htt in cells and lysates (Figures 6A and 6B). Qualitatively, the levels of Htt proteolysis are higher in the $Hdh^{111Q/111Q}$ when compared to $Hdh^{7Q/7Q}$ lines (Figure 6B). Caspases are known to cleave the Htt protein containing the polyglutamine expansion, and evidence suggests that these N-terminal cleavage products lead to cellular toxicity and apoptosis (Wellington et al., 1998). During serum withdrawal, we found that $Hdh^{111Q/111Q}$ cells have a 7-fold increase in caspase activation compared to control $Hdh^{7Q/7Q}$. Cell death occurred at 48 hr after serum withdrawal (Figure S5). All three irreversible inhibitors, **35**–**37**, at concentrations of 1–100 μM were evaluated in $Hdh^{7Q/7Q}$ and $Hdh^{111Q/111Q}$ cells and were found to significantly block caspase activity in both the normal and expanded Htt cell model 24 hr after serum deprivation (Figure 6C). Furthermore, the irreversible inhibitors **35** and **37** at concentrations of 10–100 μM blocked the proteolysis of Htt as detected by neoHtt513 (Figure 6D). Interestingly, inhibitor **36**, which incorporates additional acidic carboxylic acid functionality and thus has distinct physicochemical properties relative to inhibitors **35** and **37**, showed minimal effect. To determine the $IC_{50}$ values for inhibitors **35**–**37**, DEVDase activity was measured as a function of concentration for each inhibitor (Figure 6E). Of note, the concentration needed to block caspase activity was lower in the HD cells compared to WT. Perhaps doses of caspase inhibitors can be utilized in therapeutics that do not impact normal cellular function. We do not know the exact mechanism for the lower dose required to inhibit the caspases in the $Hdh^{111Q/111Q}$ cells, but two possible explanations are: (1) the $Hdh^{7Q/7Q}$ caspase-3 activity is from the proform of the enzyme that has a distinct $k_{cat}$ and $K_m$ when compared to active caspase-3 ($Hdh^{111Q/111Q}$ could have more); or (2) the endogenous inhibitors of caspases are lower in the HD cells due to activation of degradative pathways such as proteasome or autophagy.

Next, we evaluated these inhibitors ex vivo, using primary co-cultures of striatal and cortical neurons expressing normal and expanded Htt N-terminal fragments-Htt N90Q73, which induces degeneration of rat striatal and cortical neurons in primary co-cultures. We use co-cultures because in HD it is known that non-cell autonomous interactions and deficits in cortico-striatal circuitry occur. We use a fragment HD model because we have found that these toxic Htt fragments cause the activation of the same proteases involved in cleaving full-length Htt and producing neurotoxicity. The percentage of healthy striatal and cortical neurons after treatment with varied concentrations of the irreversible inhibitors is shown in Figure 7 (see Figure S6 for relative reversibility of neuronal effects upon removing irreversible inhibitors). All three inhibitors rescued striatal neurons from cell death, and treatment with inhibitor **35** resulted in the most significant increase of healthy striatal neurons at 0.4, 1.2, and 3.7 nM. The same trend is observed for the treatment of cortical neurons, with **35** resulting in a substantial increase (25%–175%) in healthy neurons. The control is transfection of the fluorescent protein-encoding plasmid and empty plasmid in place of Htt plasmid. For the striatal the control is 237% ± 25%. For the cortical, the control is 311% ± 60%. This suggests that some doses of the inhibitors completely rescued the cell death mediated by mutant Htt. The efficacy of the inhibitors at even single-digit nanomolar concentrations is likely due to the greater sensitivity of primary cultures to cell death when compared to the immortalized cells. Primary cultures are terminally differentiated, and the culture conditions are distinct when compared to the immortalized mouse striatal $Hdh^{7Q/7Q}$ and $Hdh^{111Q/111Q}$ cell system.

## Conclusions

The SAS method was applied to caspase-3 and -6, leading to the identification of 1,2,3-triazole-based nonpeptidic substrates with high cleavage efficiencies. Subsequent replacement of the aminocoumarin reporter group with the 2,3,5,6-tetrafluorophenoxymethyl ketone pharmacophore in the most efficient substrates led to three novel nonpeptidic irreversible inhibitors showing strong potency against caspases and weak to no

**Figure 5. Inhibitors 35–37 Block Caspase-6 or Caspase-3 Mediated Cleavage of Htt**

Full-length c-*myc*-Htt23Q and c-*myc*-Htt148Q were transiently transfected in HEK293T cells for 72 hr. Western blots of cellular lysates treated with recombinant caspase-2, -3, or -6 and inhibitors were probed with the indicated neo-specific antibody recognizing the Htt cleavage fragment. The asterisk indicates nonspecific band. The lysates contain endogenous wild-type Htt so this is also detected in the right panel in (A) and (B). For (C) it should be noted that the inhibitors are less effective on caspase-2 cleavage of Htt. Because these are cellular lysates, it is possible that addition of caspase-2 activates some of the other caspase members yielding a slight effect on full-length Htt.

See also Table S1.

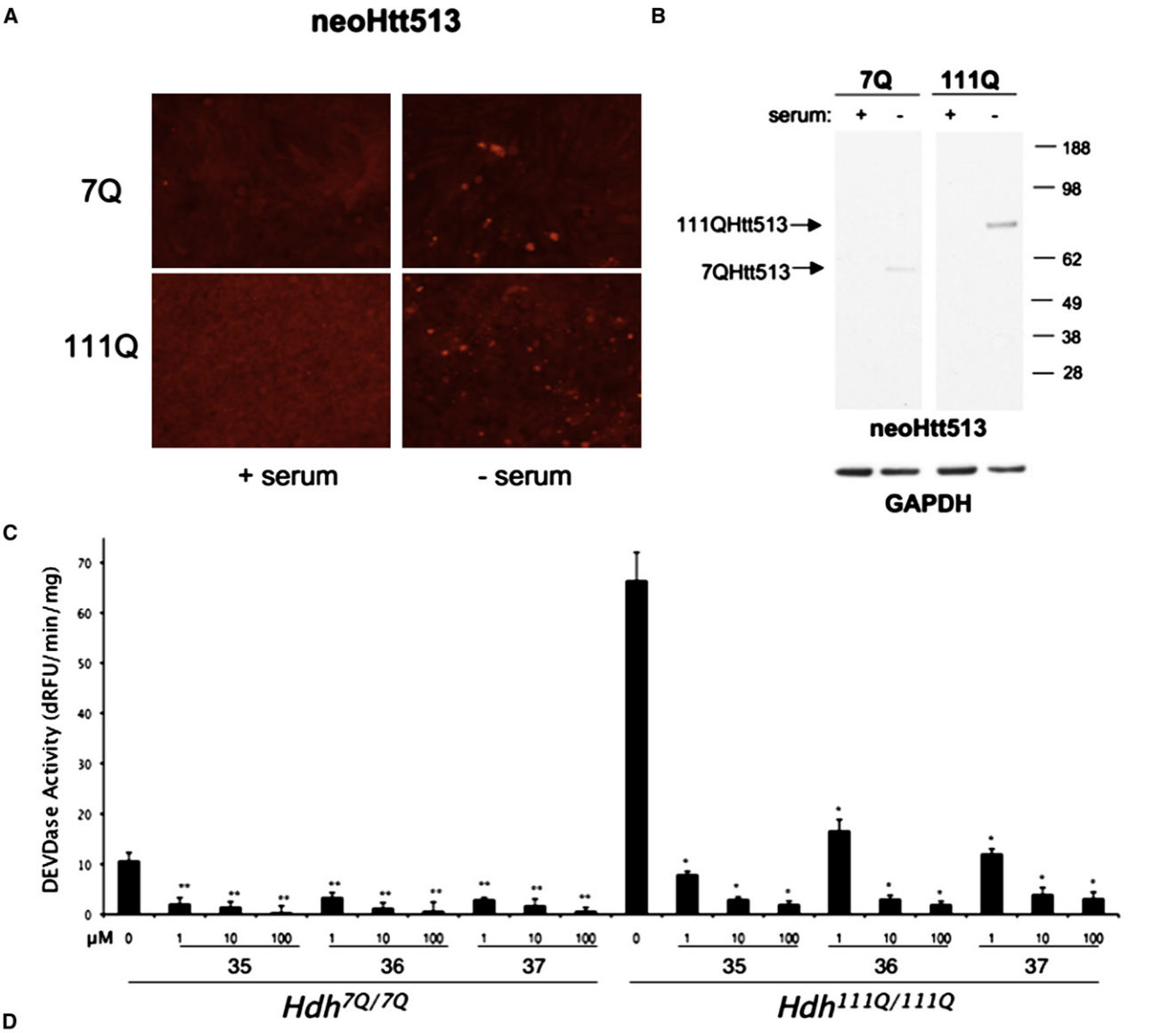


 

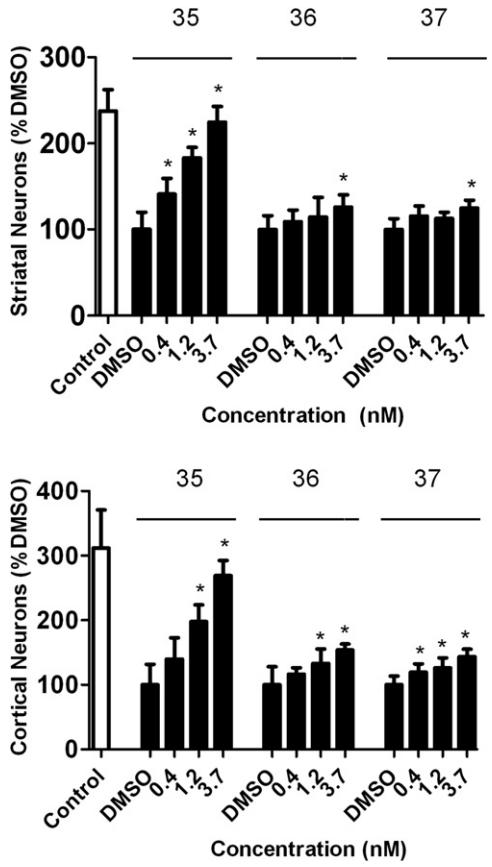


**Figure 7. Protective Effects of Caspase Inhibitors in HttN90Q73-Induced Degeneration of Rat Striatal and Cortical Neurons in Primary Co-Culture**

Rat striatal and cortical neurons expressing HttN90Q73 together with YFP or mCherry, respectively, combined in primary co-culture and treated with DMSO or caspase inhibitors at the indicated doses. YFP-positive striatal neurons and mCherry-positive cortical neurons were quantified at 6 days after transfection by automated fluorescent object detection on the Cellomics ArrayScan VTI. All conditions were normalized against the DMSO condition set to 100%. N = 6 for each condition; error bars are standard deviation. Asterisks indicate significant difference from the DMSO condition using one-way ANOVA followed by Dunnett post hoc comparison. Analysis indicates the statistical significance as: *$p < 0.05$.

inhibition of other cysteine proteases previously reported to have cross reactivity with published caspase inhibitors. All three inhibitors, **35–37**, blocked proteolysis of Htt at the caspase-3 and -6 cleavage sites, amino acids 513 and 586, respectively. Moreover, in a HD model, all three inhibitors rescued cell death in striatal and cortical neurons at nanomolar concentrations. These pan-caspase inhibitors continue to be applied as tool compounds in studies of Htt proteolysis and toxicity. Future work will be directed at evaluating these compounds in mouse models of HD to determine their effect on the pathogenesis of HD.

## SIGNIFICANCE

**HD is an incurable disease caused by a mutation encoding a polyglutamine expansion in the N terminus of the huntingtin protein. Major research efforts have focused on the relationship of polyglutamine repeats and HD pathogenesis. Proposed mechanisms leading to neuronal dysfunction and death include formation of polyglutamine aggregates and inclusions (Arrasate et al., 2004; Sawada et al., 2007), altered confirmation of mutant huntingtin leading to transcriptional dysregulation (Dunah et al., 2002; Li et al., 2002; Zhai et al., 2005), excitotoxic neuron damage by excessive stimulation of glutamate receptors (Charvin et al., 2008; Fan et al., 2007; Stack et al., 2007), and induction of apoptosis and proteolysis. Evidence has emerged that suggest Htt fragments lead to neuronal toxicity, but the exact mechanism remains unknown. The proteolytic cleavage of Htt and the enzymes involved in this process have emerged as potential therapeutic targets for treating HD.**

**Caspases are proteases involved in programmed cell death and have been found to cleave Htt. Specifically, accumulation of caspase-cleaved Htt fragments represents a neuropathological hallmark of HD. Furthermore, Graham et al. (2006) showed that mice expressing mutant Htt resistant to cleavage by caspase-6, and not caspase-3, exhibit normal neuronal function and do not develop neurodegeneration. Therefore, inhibitors that block caspase cleavage provide a promising starting point for the study of Htt proteolysis.**

**A substrate-based fragment approach was used to develop three nonpeptidic irreversible inhibitors displaying pan-caspase activity. In vitro, these inhibitors blocked Htt cleavage by caspase-3 and -6. Results from a HD cellular toxicity model showed that all three inhibitors dramatically blocked caspase activation in disease model cells. Ex vivo studies using cultures of striatal and cortical neurons expressing mutant Htt demonstrated the rescue of neuronal death after treatment with the inhibitors. Overall, the**

**Figure 6. Inhibitors 35–37 Block Caspase Activation in Mouse Striatal *Hdh*$^{7Q/7Q}$ and *Hdh*$^{111Q/111Q}$ Cells**

(A) Striatal *Hdh*$^{7Q/7Q}$ and *Hdh*$^{111Q/111Q}$ cells were cultured for 48 hr and then subjected to analysis 24 hr after serum withdrawal. Immunochemistry of *Hdh*$^{7Q/7Q}$ and *Hdh*$^{111Q/111Q}$ cells with neoHtt513 demonstrates cleavage of Htt. Qualitatively, more Htt cleavage is found in the *Hdh*$^{111Q/111Q}$ cells.

(B) Western blot analysis using neoHtt513 antibody demonstrates proteolysis of Htt at the caspase-3 cleavage site located at amino acid 513 after serum withdrawal.

(C) Striatal *Hdh*$^{7Q/7Q}$ and *Hdh*$^{111Q/111Q}$ cells where cultured for 48 hr and then caspase activity was measured 24 hr after serum withdrawal. *Hdh*$^{111Q/111Q}$ cells have a 7-fold increase in caspase activation compared to control *Hdh*$^{7Q/7Q}$. Inhibitors **35–37** blocked caspase activity at the doses indicated. The experiments were repeated three times, each time with an n = 3. ANOVA analysis indicates the statistical significance: *$p < 0.05$, **$p < 0.01$, and ***$p < 0.005$.

(D) Striatal *Hdh*$^{7Q/7Q}$ and *Hdh*$^{111Q/111Q}$ cells were cultured for 48 hr. Then, 24 hr after serum withdrawal cell lysates were prepared. Inhibitors **35–37** blocked the proteolysis of Htt at the caspase-3 cleavage site located at amino acid 513 at the indicated doses.

See also Figures S5 and S6.

**identified inhibitors have validated the correlation between blocking caspase Htt cleavage and rescue of HD-mediated neurodegeneration.**

## EXPERIMENTAL PROCEDURES

### Fluorogenic Substrate Screen against Caspase-3 and -6

Caspase-3 and -6–9 were obtained by expression in *E. coli* as previously described (Stennicke and Salvesen, 1999). Caspase-1, cathepsin B, L, and V were purchased from EMD Biosciences (San Diego, CA, USA), caspase-2 was purchased from Biomol International (Plymouth Meeting, PA, USA), and Legumain was purchased from R&D Systems (Minneapolis, MN, USA). Assays were conducted at 37°C in duplicate with and without the enzyme in Dynatech Microfluor fluorescence 96 well microtiter plates, and readings were taken on a Molecular Devices Spectra Max Gemini XS instrument according to previously reported protocols (see Supplemental Experimental Procedures for full assay details for each enzyme). Caspases 3 and 6 were used at concentrations 2.7 and 3.0 μM, respectively. Relative fluorescent units (RFU) were measured at regular intervals over a period of time (maximum 15 min). A plot of RFU versus time was made for each substrate with and without enzyme. The slope of the plotted line gave relative $k_{cat}/K_m$ of each substrate.

### Inhibitor Kinetic Assays

Caspase substrates Ac-DEVD-AMC (caspases 3 and 6–8), Ac-VDVAD-AFC (caspase-2), and Ac-LEHD-AFC (caspase-9) were purchased from EMD Biosciences, and Ac-VDVAD-AMC (caspase-2) was purchased from Biomol International. Cathepsins B and V substrate Cbz-FR-AMC was purchased from EMD Biosciences. Cathepsin S substrate Cbz-LR-AMC and legumain substrate Cbz-AAN-AMC were purchased from Bachem (Torrance, CA, USA). Assay wells contained a mixture of inhibitor and substrate in buffer (see Supplemental Experimental Procedures for full assay details for each enzyme). Aliquots of enzyme were added to each well to initiate the assay. Hydrolysis of the fluorescent substrate was monitored fluorometrically for 45 min. The $k_{inact}/K_i$ for inhibitors was determined under pseudo-first order conditions using the progress curve method (Bieth, 1995; Ekici et al., 2006). Inhibition was measured in triplicate, and the average and standard deviation is reported. Detailed procedures for each enzyme, including buffer conditions and enzyme, inhibitor and substrate concentrations, are provided in the first Supplemental Experimental Procedures.

### Htt Neoepitope Antibody Production

Antibodies specific for the C-terminal ends of Htt caspase cleavage products ending at amino acid 513, 552, and 586 were prepared using the immunizing peptides KLH-DHTLQADSVD, KLH-DSDPAMDLND, and KLH-COSDSSEIVLD. Peptide sequences were injected into rabbits, antibody was purified to the injected peptide, and a bridging peptide was used to remove antibodies reacting to full-length Htt (Open Biosystems). Antibodies were affinity purified as previously described with minor modifications (Wellington et al., 2002; Gervais et al., 1999).

### Htt Constructs

Htt expression constructs used in these studies included a normal (23Q) and expanded (148Q) full-length Htt construct.

### Cell Culture

SuperFect reagent (QIAGEN) was used for transient transfections of human embryonic kidney (HEK) 293T cells with Htt constructs. Cells were collected 60 hr after transfection for analysis. 293T cells or striatal $Hdh^{7Q/7Q}$ and $Hdh^{111Q/111Q}$ cells were cultured in Dulbecco's modified eagle medium (DMEM; Cellgro) with 10% fetal bovine serum (FBS) and 100 U/ml penicillin and 100 μg/ml streptomycin.

### Western Analysis

293T cell pellets were lysed in M-PER (Mammalian Protein Extraction Reagent, Pierce) with protease inhibitors (Mini Complete, Roche), lysates were sonicated and then spun to remove debris (16,000 × *g*, 20 min). Protein concentration was determined by a BCA Protein Assay kit (Pierce). Htt-expressing lysates were in some cases treated exogenously with caspases 2, 3, or 6 (ENZO, 100 U, 2 hr, 37°C) with and without inhibitors **35**–**37**. Samples were resolved by SDS-PAGE on NuPAGE 4–12% BisTris gel (Invitrogen) in MES running buffer (Invitrogen) for 55 min at 200 V. Proteins were transferred to Optitran BA-S nitrocellulose (Schleicher & Schuell) for 14 hr at 20 V at 4°C. Membranes were blocked in 5% milk in Tris-buffered saline Tween-20 and probed overnight at 4°C with polyclonal neoHtt513, neoHtt552, and neoHtt586 (Open Biosystems; 1:1000 or 1:100, produced in collaboration with CHDI/Open Biosystems) or monoclonal α-Huntingtin 2166 (Chemicon; 1:1000). Secondary anti-rabbit or anti-mouse antibodies (1:3000; Amersham Biosciences/GE Healthcare) and enhanced chemiluminescence (ECL) reagent (Pierce) were used for detection. We utilized anti-GAPDH as the loading control (Fitzgerald No. 10R-G109a; 1:1000).

### $k_{cat}/K_m$ of Htt with Caspases

293T cells overexpressing myc-tagged 23Q human full-length Htt were lysed in M-PER (Mammalian Protein Extraction Reagent, Pierce), sonicated and spun to remove debris (16,000 × *g*, 20 min). Protein was determined using a BCA assay kit (Pierce). Purified human poly-(ADP-ribose) polymerase (PARP) was obtained from Trevigen (Gaithersburg, MD, USA). Htt lysate (15 μg) was incubated with caspase-3 (4 nM; ENZO) or caspase-6 (48 nM; ENZO) for 60 min at 37°C in caspase assay buffer (20 mM PIPES [pH 7.2], 100 mM NaCl, 1% CHAPS, 10% sucrose). Purified PARP (35 ng) was incubated with caspase-3 (7.2–144 nM) under identical conditions. NuPAGE LDS sample buffer (Invitrogen) and 50 mM DTT were added, and samples were boiled and separated using SDS-PAGE. Following transfer to nitrocellulose membranes, Htt protein blots were incubated in monoclonal Htt 2166 (1:500; Millipore), PARP protein blots were incubated in polyclonal PARP 253 (1:300; ENZO), and densitometry of bands was performed. All reactions were carried out using subsaturating levels of substrate, where the cleavage is assumed to be a first-order process. Values of $k_{cat}/K_m$ were calculated from the relationship $S_t/S_o = e^{-kobs*t}$, where $S_t$ = concentration of substrate remaining at time $t$, $S_o$ = initial substrate concentration, and $k_{obs} = k_{cat}*[enzyme]/K_m$ (Gervais et al., 1998).

### Caspase Activity in Striatal $Hdh^{7Q/7Q}$ and $Hdh^{111Q/111Q}$ Cells

Striatal $Hdh^{7Q/7Q}$ and $Hdh^{111Q/111Q}$ cells were maintained at 33°C in a humidified atmosphere of 95% air and 5% $CO_2$, in DMEM supplemented with 10% FBS, 100 U/ml penicillin, and 100 μg/ml streptomycin. Cells were fed with fresh media every 2–3 d. Striatal cells were plated at 5000 cells/well in collagen-coated 96 well plates and were grown for 48 hr. Cells were maintained in serum DMEM for 24 hr with or without caspase inhibitors and an additional 24 hr without serum with same inhibitor treatment. Caspase 3/7 activity was measured using the APO3 HTS kit per manufacturer's direction (Mountain View, CA, USA) and normalized by protein concentration. Briefly, cells were lysed in working cell lysis buffer (50 μl, 1:1 lysis buffer: serum-free DMEM) by shaking at 700 rpm for 5 min, and a 20 μl aliquot was measured for protein concentration. Afterward, 70 μl of working lysis buffer with DTT (15 mM), and caspase substrate (1×) was added to remaining lysed cells, shaken briefly, and read continuously at 37°C for 90 min with excitation at 488 nm and emission at 530 nm.

### Immunocytochemistry

Striatal $Hdh^{7Q/7Q}$ and $Hdh^{111Q/111Q}$ cells cultured on coverslips with or without serum withdrawal were fixed with 4% paraformaldehyde for 20 min at room temperature. The fixed cells were then permeabilized with 0.1% Triton X-100 for 10 min and blocked with 5% donkey serum for 45 min. The incubation with the primary antibody (rabbit polyclonal neoHtt513, 1:100) at 4°C overnight was followed by secondary antibody (donkey anti rabbit Alexa546, 1:1000; Invitrogen) incubation at room temperature for 1.5 hr. Finally, cells were mounted to a slide with droplets of Prolong Gold with DAPI (Invitrogen) on it before microscopy.

### Primary Cortico-Striatal Co-Culture

Striatum and cortex from E18 rat embryos were microdissected, enzymatically treated with papain, and dissociated. Five million cells of each type were electroporated separately (Amaxa Biosystems) with DNA constructs expressing either YFP in striatal neurons or mCherry in cortical neurons together with a plasmid expressing mutant polyQ expanded Htt exon1 (HttN90Q73), then

plated together on a layer of astrocytes that was prepared 3 days prior. Our method for assessing culture health in experiments is by determining the number and morphology of GFP-expressing cells. In developing the assay we found with vital stains that about 50% of cells die immediately after the electroporation. The neurons that survive the electroporation appear to be healthy, extending neurites and forming functional synapses, as assessed by synaptic marker staining and electrophysiology (Kaltenbach et al., 2010). Neurons and astrocytes were grown in Neurobasal media (Invitrogen) supplemented with 5% fetal calf serum (Sigma), 2 mM glutamine (GlutaMAX; Invitrogen), 10 mM potassium chloride, and 5 μg/ml gentamycin. Astrocytes were isolated from E18 embryos and expanded for three passages before plating into 96 well plates. Co-cultures were incubated in 95% $O_2$/5% $CO_2$ at 37°C for 6 days before analysis. Compounds were dissolved in DMSO and dosed as a single dose shortly after neuron plating. The control condition was HttN90Q73 with DMSO alone. For quantification of neurons using the Cellomics ArrayScan VTI, fluorescent images were acquired at 10× magnification from nine fields per well using YFP and dsRED filter sets and analyzed using the Target Activation algorithm. The algorithm was optimized for object size, object shape, and fluorescence intensity to identify specific neuron cell bodies. Healthy neurons are easily identified by the size of the cell body and neuritic morphology. Graphical analysis and statistical computations were performed with GraphPad Prism.

## SUPPLEMENTAL INFORMATION

Supplemental Information includes Supplemental Experimental Procedures, six figures, and one table and can be found with this article online at doi:10.1016/j.chembiol.2010.08.014.

## ACKNOWLEDGMENTS

This research was supported by grants from NIH: GM54051 (J.A.E.), NS40251 (L.M.E.), CHDI (L.M.E. and D.C.L.), and RGP0024/2006 from the Human Frontier Science Program (G.S.S.). Neo Htt epitopes were produced in collaboration with Jacqueline Duke and Matt Baker at OpenBiosystems. We thank both of them for their expert advice and help.

Received: November 25, 2009
Revised: August 30, 2010
Accepted: August 31, 2010
Published: November 23, 2010

## REFERENCES

Arrasate, M., Mitra, S., Schweitzer, E.S., Segal, M.R., and Finkbeiner, S. (2004). Inclusion body formation reduces levels of mutant huntingtin and the risk of neuronal death. Nature *431*, 805–810.

Baskin-Bey, E.S., Washburn, K., Feng, S., Oltersdorf, T., Shapiro, D., Huyghe, M., Burgart, L., Garrity-Park, M., van Vilsteren, F.G.I., Oliver, L.K., et al. (2007). Clinical trial of the pan-caspase inhibitor, IDN-6556, in human liver preservation injury. Am. J. Transplant. *7*, 218–225.

Bieth, J.G. (1995). Theoretical and practical aspects of proteinase inhibition kinetics. Methods Enzymol. *248*, 59–84.

Brak, K., Doyle Patricia, S., McKerrow James, H., and Ellman Jonathan, A. (2008). Identification of a new class of nonpeptidic inhibitors of cruzain. J. Am. Chem. Soc. *130*, 6404–6410.

Brik, A., Alexandratos, J., Lin, Y.-C., Elder John, H., Olson Arthur, J., Wlodawer, A., Goodsell David, S., and Wong, C.-H. (2005). 1,2,3-triazole as a peptide surrogate in the rapid synthesis of HIV-1 protease inhibitors. ChemBioChem *6*, 1167–1169.

Charvin, D., Roze, E., Perrin, V., Deyts, C., Betuing, S., Pages, C., Regulier, E., Luthi-Carter, R., Brouillet, E., Deglon, N., et al. (2008). Haloperidol protects striatal neurons from dysfunction induced by mutated huntingtin in vivo. Neurobiol. Dis. *29*, 22–29.

Chen, M., Ona, V.O., Li, M., Ferrante, R.J., Fink, K.B., Zhu, S., Bian, J., Guo, L., Farrell, L.A., Hersch, S.M., et al. (2000). Minocycline inhibits caspase-1 and caspase-3 expression and delays mortality in a transgenic mouse model of Huntington disease. Nat. Med. *6*, 797–801.

Cornelis, S., Kersse, K., Festjens, N., Lamkanfi, M., and Vandenabeele, P. (2007). Inflammatory caspases: targets for novel therapies. Curr. Pharm. Des. *13*, 367–385.

Davies, S.W., Turmaine, M., Cozens, B.A., DiFiglia, M., Sharp, A.H., Ross, C.A., Scherzinger, E., Wanker, E.E., Mangiarini, L., and Bates, G.P. (1997). Formation of neuronal intranuclear inclusions underlies the neurological dysfunction in mice transgenic for the HD mutation. Cell *90*, 537–548.

DiFiglia, M., Sapp, E., Chase, K.O., Davies, S.W., Bates, G.P., Vonsattel, J.P., and Aronin, N. (1997). Aggregation of huntingtin in neuronal intranuclear inclusions and dystrophic neurites in brain. Science *277*, 1990–1993.

Dunah, A.W., Jeong, H., Griffin, A., Kim, Y.-M., Standaert, D.G., Hersch, S.M., Mouradian, M.M., Young, A.B., Tanese, N., and Krainc, D. (2002). Sp1 and TAFII 130 transcriptional activity disrupted in early Huntington's disease. Science *296*, 2238–2243.

Ekici, O.D., Li, Z.Z., Campbell, A.J., James, K.E., Asgian, J.L., Mikolajczyk, J., Salvesen, G.S., Ganesan, R., Jelakovic, S., Grütter, M.G., and Powers, J.C. (2006). Design, synthesis, and evaluation of aza-peptide Michael acceptors as selective and potent inhibitors of caspases-2, -3, -6, -7, -8, -9, and -10. J. Med. Chem. *49*, 5728–5749.

Fan, M.M.Y., Fernandes, H.B., Zhang, L.Y.J., Hayden, M.R., and Raymond, L.A. (2007). Altered NMDA receptor trafficking in a yeast artificial chromosome transgenic mouse model of Huntington's disease. J. Neurosci. *27*, 3768–3779.

Gafni, J., and Ellerby, L.M. (2002). Calpain activation in Huntington's disease. J. Neurosci. *22*, 4842–4849.

Gafni, J., Hermel, E., Young, J.E., Wellington, C.L., Hayden, M.R., and Ellerby, L.M. (2004). Inhibition of calpain cleavage of huntingtin reduces toxicity: accumulation of calpain/caspase fragments in the nucleus. J. Biol. Chem. *279*, 20211–20220.

Gervais, F.G., Thornberry, N.A., Ruffolo, S.C., Nicholson, D.W., and Roy, S. (1998). Caspases cleave focal adhesion kinase during apoptosis to generate a FRNK-like polypeptide. J. Biol. Chem. *273*, 17102–17108.

Gervais, F.G., Xu, D., Robertson, G.S., Vaillancourt, J.P., Zhu, Y., Huang, J., LeBlanc, A., Smith, D., Rigby, M., Shearman, M.S., et al. (1999). Involvement of caspases in proteolytic cleavage of Alzheimer's amyloid-beta precursor protein and amyloidogenic A beta peptide formation. Cell *97*, 395–406.

Goldberg, Y.P., Nicholson, D.W., Rasper, D.M., Kalchman, M.A., Koide, H.B., Graham, R.K., Bromm, M., Kazemi-Esfarjani, P., Thornberry, N.A., Vaillancourt, J.P., and Hayden, M.R. (1996). Cleavage of huntingtin by apopain, a proapoptotic cysteine protease, is modulated by the polyglutamine tract. Nat. Genet. *13*, 442–449.

Graham, R.K., Deng, Y., Slow, E.J., Haigh, B., Bissada, N., Lu, G., Pearson, J., Shehadeh, J., Bertram, L., Murphy, Z., et al. (2006). Cleavage at the caspase-6 site is required for neuronal dysfunction and degeneration due to mutant huntingtin. Cell *125*, 1179–1191.

Gutekunst, C.-A., Li, S.-H., Yi, H., Mulroy, J.S., Kuemmerle, S., Jones, R., Rye, D., Ferrante, R.J., Hersch, S.M., and Li, X.-J. (1999). Nuclear and neuropil aggregates in Huntington's disease: relationship to neuropathology. J. Neurosci. *19*, 2522–2534.

HDCRG (The Huntington's Disease Collaborative Research Group). (1993). A novel gene containing a trinucleotide repeat that is expanded and unstable on Huntington's disease chromosomes. Cell *72*, 971–983.

Hermel, E., Gafni, J., Propp, S.S., Leavitt, B.R., Wellington, C.L., Young, J.E., Hackam, A.S., Logvinova, A.V., Peel, A.L., Chen, S.F., et al. (2004). Specific caspase interactions and amplification are involved in selective neuronal vulnerability in Huntington's disease. Cell Death Differ. *11*, 424–438.

Inagaki, H., Tsuruoka, H., Hornsby, M., Lesley Scott, A., Spraggon, G., and Ellman Jonathan, A. (2007). Characterization and optimization of selective, nonpeptidic inhibitors of cathepsin S with an unprecedented binding mode. J. Med. Chem. *50*, 2693–2699.

Kaltenbach, L.S., Bolton, M.M., Shah, B., Kanju, P.M., Lewis, G.M., Turmel, G.J., Whaley, J.C., Trask, O.J., Jr, and Lo, D.C. (2010). Composite primary neuronal high-content screening assay for Huntington's disease incorporating non-cell-autonomous interactions. Biomol. Screen *15*, 806–819.

Li, S.H., Cheng, A.L., Zhou, H., Lam, S., Rao, M., Li, H., and Li, X.J. (2002). Interaction of Huntington disease protein with transcriptional activator Sp1. Mol. Cell. Biol. *22*, 1277–1287.

Linton, S.D., Aja, T., Allegrini, P.R., Deckwerth, T.L., Diaz, J.-L., Hengerer, B., Herrmann, J., Jahangiri, K.G., Kallen, J., Karanewsky, D.S., et al. (2004). Oxamyl dipeptide caspase inhibitors developed for the treatment of stroke. Bioorg. Med. Chem. Lett. *14*, 2685–2691.

Linton, S.D., Aja, T., Armstrong, R.A., Bai, X., Chen, L.S., Chen, N., Ching, B., Contreras, P., Diaz, J.L., Fisher, C.D., et al. (2005). First-in-class pan caspase inhibitor developed for the treatment of liver disease. J. Med. Chem. *48*, 6779–6782.

Lunkes, A., Lindenberg, K.S., Ben-Haiem, L., Weber, C., Devys, D., Landwehrmeyer, G.B., Mandel, J.L., and Trottier, Y. (2002). Proteases acting on mutant huntingtin generate cleaved products that differentially build up cytoplasmic and nuclear inclusions. Mol. Cell *10*, 259–269.

Martindale, D., Hackam, A., Wieczorek, A., Ellerby, L., Wellington, C., McCutcheon, K., Singaraja, R., Kazemi-Esfarjani, P., Devon, R., Kim, S.U., et al. (1998). Length of huntingtin and its polyglutamine tract influences localization and frequency of intracellular aggregates. Nat. Genet. *18*, 150–154.

O'Brien, T., and Lee, D. (2004). Prospects for caspase inhibitors. Mini Rev. Med. Chem. *4*, 153–165.

Patterson, A.W., Wood, W.J.L., Hornsby, M., Lesley, S., Spraggon, G., and Ellman, J.A. (2006). Identification of selective, nonpeptidic nitrile inhibitors of cathepsin S using the substrate activity screening method. J. Med. Chem. *49*, 6298–6307.

Pop, C., and Salvesen, G.S. (2009). Human caspases: activation, specificity, and regulation. J. Biol. Chem. *284*, 21777–21781.

Reed, J.C. (2002). Apoptosis-based therapies. Nat. Rev. Drug Discov. *1*, 111–121.

Rozman-Pungercar, J., Kopitar-Jerala, N., Bogyo, M., Turk, D., Vasiljeva, O., Stefe, I., Vandenabeele, P., Broemme, D., Puizdar, V., Fonovic, M., et al. (2003). Inhibition of papain-like cysteine proteases and legumain by caspase-specific inhibitors: when reaction mechanism is more important than specificity. Cell Death Differ. *10*, 881–888.

Sawada, H., Ishiguro, H., Nishii, K., Yamada, K., Tsuchida, K., Takahashi, H., Goto, J., Kanazawa, I., and Nagatsu, T. (2007). Characterization of neuron-specific huntingtin aggregates in human huntingtin knock-in mice. Neurosci. Res. *57*, 559–573.

Schulz, J.B., Weller, M., Matthews, R.T., Heneka, M.T., Groscurth, P., Martinou, J.C., Lommatzsch, J., Von Coelln, R., Wullner, U., Loschmann, P.A., et al. (1998). Extended therapeutic window for caspase inhibition and synergy with MK-801 in the treatment of cerebral histotoxic hypoxia. Cell Death Differ. *5*, 847–857.

Schweizer, A., Briand, C., and Gruetter, M.G. (2003). Crystal structure of xaspase-2, apical initiator of the intrinsic apoptotic pathway. J. Biol. Chem. *278*, 42441–42447.

Sexton, K.B., Witte, M.D., Blum, G., and Bogyo, M. (2007). Design of cell-permeable, fluorescent activity-based probes for the lysosomal cysteine protease asparaginyl endopeptidase (AEP)/legumain. Bioorg. Med. Chem. Lett. *17*, 649–653.

Stack, E.C., Dedeoglu, A., Smith, K.M., Cormier, K., Kubilus, J.K., Bogdanov, M., Matson, W.R., Yang, L., Jenkins, B.G., Luthi-Carter, R., et al. (2007). Neuroprotective effects of synaptic modulation in Huntington's disease R6/2 mice. J. Neurosci. *27*, 12908–12915.

Stennicke, H.R., and Salvesen, G.S. (1999). Caspases: preparation and characterization. Methods *17*, 313–319.

Talanian, R.V., Quinlan, C., Trautz, S., Hackett, M.C., Mankovich, J.A., Banach, D., Ghayur, T., Brady, K.D., and Wong, W.W. (1997). Substrate specificities of caspase family proteases. J. Biol. Chem. *272*, 9677–9682.

Thornberry, N.A., Rano, T.A., Peterson, E.P., Rasper, D.M., Timkey, T., Garcia-Calvo, M., Houtzager, V.M., Nordstrom, P.A., Roy, S., Vaillancourt, J.P., et al. (1997). A combinatorial approach defines specificities of members of the caspase family and granzyme B. Functional relationships established for key mediators of apoptosis. J. Biol. Chem. *272*, 17907–17911.

Toulmond, S., Tang, K., Bureau, Y., Ashdown, H., Degen, S., O'Donnell, R., Tam, J., Han, Y., Colucci, J., Giroux, A., et al. (2004). Neuroprotective effects of M826, a reversible caspase-3 inhibitor, in the rat malonate model of Huntington's disease. Br. J. Pharmacol. *141*, 689–697.

Trettel, F., Rigamonti, D., Hilditch-Maguire, P., Wheeler, V.C., Sharp, A.H., Persichetti, F., Cattaneo, E., and MacDonald, M.E. (2000). Dominant phenotypes produced by the HD mutation in STHdh(Q111) striatal cells. Hum. Mol. Genet. *9*, 2799–2809.

Wellington, C.L., Ellerby, L.M., Hackam, A.S., Margolis, R.L., Trifiro, M.A., Singaraja, R., McCutcheon, K., Salvesen, G.S., Propp, S.S., Bromm, M., et al. (1998). Caspase cleavage of gene products associated with triplet expansion disorders generates truncated fragments containing the polyglutamine tract. J. Biol. Chem. *273*, 9158–9167.

Wellington, C.L., Singaraja, R., Ellerby, L., Savill, J., Roy, S., Leavitt, B., Cattaneo, E., Hackam, A., Sharp, A., Thornberry, N., et al. (2000). Inhibiting caspase cleavage of huntingtin reduces toxicity and aggregate formation in neuronal and nonneuronal cells. J. Biol. Chem. *275*, 19831–19838.

Wellington, C.L., Ellerby, L.M., Gutekunst, C.A., Rogers, D., Warby, S., Graham, R.K., Loubser, O., van Raamsdonk, J., Singaraja, R., Yang, Y.Z., et al. (2002). Caspase cleavage of mutant huntingtin precedes neurodegeneration in Huntington's disease. J. Neurosci. *22*, 7862–7872.

Wood, W.J.L., Patterson, A.W., Tsuruoka, H., Jain, R.K., and Ellman, J.A. (2005). Substrate activity screening: a fragment-based method for the rapid identification of nonpeptidic protease inhibitors. J. Am. Chem. Soc. *127*, 15521–15527.

Zhai, W., Jeong, H., Cui, L., Krainc, D., and Tjian, R. (2005). In vitro analysis of Huntingtin-mediated transcriptional repression reveals multiple transcription factor targets. Cell *123*, 1241–1253.

 